

# Dislocation Microstructure and Internal-Stress Measurements by Convergent-Beam Electron Diffraction on Creep-Deformed Cu and Al

M.E. KASSNER, M.T. PÉREZ-PRADO, M. LONG, and K.S. VECCHIO

Creep experiments were conducted on aluminum single crystals and copper polycrystals deformed within the five-power-law regime. The dislocation structure of copper, which has not been extensively characterized in the past, consists of less-well-defined subgrain walls of relatively low misorientation, typically between 0.1 and 0.3 deg, with a Frank network of dislocations within the subgrains. The aluminum, as expected, consisted of well-defined subgrain boundaries with a typical misorientation between 1.0 and 2.0 deg. The subgrains were probed from one boundary to another in copper and aluminum using convergent-beam electron diffraction (CBED). This allowed a determination of any changes in the lattice parameter, which would indicate the presence of any internal stresses. Earlier investigations by others suggested that internal stresses may be high in the vicinity of the “hard” subgrain boundaries in both loaded and unloaded specimens, based on a variety of techniques including X-ray diffraction (XRD), stress-dip tests, as well as some preliminary CBED. It was determined in this work that the lattice parameter was unchanged at the equilibrium or stress-free value within the interior of the subgrains and along (within a one-beam diameter) the subgrain boundaries.

## I. INTRODUCTION

THE purpose of this research is twofold. One objective is to characterize the dislocation substructure of copper deformed with the five-power-law regime. The second and primary objective is an investigation of the existence of internal stresses in creep-deformed Cu and Al.

### A. Creep of Copper

Cu was investigated in the past, and it appears that this material obeys a classic five-power-law behavior. Figure 1 reflects much of the early creep work on Cu.<sup>[1–8]</sup> Several conclusions were apparent from the early work. Usually, the activation energy for metals and alloys over the five-power-law regime corresponds to lattice self-diffusion, and a decrease in the activation energy for creep is observed during power-law breakdown (PLB)<sup>[9]</sup> at roughly 0.5 to 0.6  $T_m$ . It has often been suggested that, within PLB, the decrease in  $Q_c$  corresponds to a switch to dislocation pipe diffusion with an activation energy of  $Q_p$ . The rate-controlling mechanism for creep is still dislocation climb. In the case of Cu, the same

arguments by Barrett *et al.*<sup>[2,3]</sup> have been applied, except that the transition to climb control by vacancy diffusion *via* dislocation pipes occurs at relatively high temperatures well within five-power-law behavior, at 0.7  $T_m$ . More recent work by Raj and Langdon<sup>[6]</sup> suggests that there is a more gradual and less dramatic decrease in  $Q_c$  that is approximately equal to  $Q_{sd}$  over the entire five-power-law regime. Curiously, in Figure 1, *both* the data above and below 0.7  $T_m$  are reasonably described by five-power-law behavior using a single activation energy,  $Q_{sd}$ . The PLB in Figure 1 occurs at about that combination of temperature and strain-rate expected, according to Sherby and Burke.<sup>[38]</sup>

It is recognized that creep experiments using copper are difficult for at least two reasons. One is that discontinuous dynamic recrystallization (DRX) easily occurs at higher temperatures within five-power-law creep.<sup>[2,5,10]</sup> Thus, restoration can occur by mechanisms other than just dynamic recovery, as with five-power-law creep. Second, oxide particles can form unless *both* the annealing conditions utilize sufficient vacuum levels and the testing conditions are sufficiently inert.<sup>[2]</sup> These particles can cause early fracture and preclude sufficient strain to achieve a genuine steady state, which is a balance between hardening processes and dynamic recovery. The particles could also lead to dislocation configurations nonreflective of the pure metal. This study consisted of deforming copper at temperatures below that suggested for DRX, which was then annealed at high vacuum and tested in an inert atmosphere. This allowed an assessment of the lower-temperature five-power-law creep behavior and, especially, an evaluation of the steady-state dislocation substructure. Some of the most frequently referenced Cu creep work suggests that well-defined subgrains do *not* form in pure Cu and, unlike most metals in the five-power-law regime, cellular tangles of dislocations form instead.<sup>[11]</sup> Others<sup>[4,8,12,13]</sup> appear to suggest that subgrains form, although the micrographs can be ambiguous. Terms such as “cells,” “subcells,” “subgrains,” “poorly developed

M.E. KASSNER, Northwest Aluminum Professor, Department of Mechanical Engineering, Oregon State University, Corvallis, OR 97331, is Adjunct Professor, Mechanical and Aerospace Engineering Department, University of California at San Diego, La Jolla, CA 92093-0411. M.T. PÉREZ-PRADO, Researcher, CENIM, CSIC, Madrid, Spain, is Research Associate, Mechanical and Aerospace Engineering Department, University of California at San Diego. M. LONG, formerly Research Assistant, Department of Mechanical Engineering, Oregon State University, is Engineer at Hewlett Packard, Corvallis, OR 97331, and K.S. VECCHIO, Professor, is with the Mechanical and Aerospace Engineering Department, University of California at San Diego.

This article is based on a presentation made in the workshop entitled “Mechanisms of Elevated Temperature Plasticity and Fracture,” which was held June 27–29, 2001, in San Diego, CA, concurrent with the 2001 Joint Applied Mechanics and Materials Summer Conference. The workshop was sponsored by Basic Energy Sciences of the United States Department of Energy.

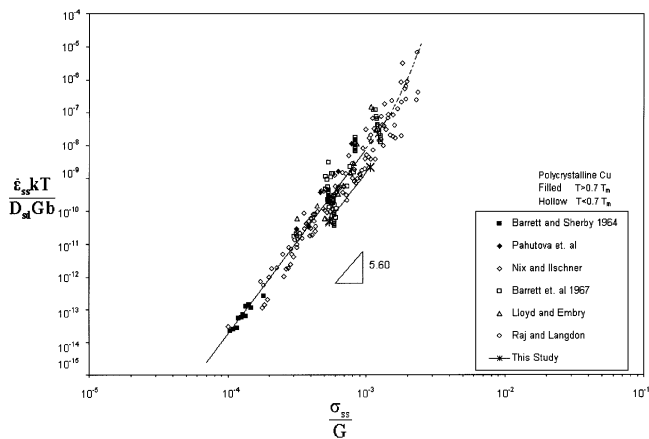


Fig. 1—The modulus compensated steady-state stress vs the (lattice self-) diffusion coefficient compensated steady-state strain rate of pure copper.

subgrains,” and “less-well-defined subgrains” are all used to describe the heterogeneous dislocation substructure. This description or analysis has implications toward the second aspect of this study, internal stresses.

### B. Internal Stresses

The second objective of this work recognizes that one of the important concepts over the past few decades within the creep community is that of the internal stress (or backstress), which, of course, has been suggested for cyclic deformation as well. Understanding creep at a fundamental level requires a resolution as to whether internal stresses or backstresses exist. The concept of internal stresses or backstresses in materials may have first been discussed in connection with the Bauschinger effect, which is observed both at high and low temperatures in cyclic deformation. Here, the metal strain hardens after some plastic straining, and on reversal of the direction of straining, the metal plastically flows at a stress less in magnitude than in the forward direction, in contrast to what would be expected based on isotropic hardening. Not only is the flow stress lower on reversal, but also the early hardening features are different as well.

Sleeswyk *et al.*<sup>[14]</sup> analyzed the hardening features in several materials cyclically deformed at ambient temperature and found that the hardening behavior on reversal can be modeled by that of the monotonic case, provided a small (*e.g.*, 0.01) “reversible” strain is subtracted from the early plastic strain associated with each reversal. This led Sleeswyk and co-workers to conclude an Orowan-type mechanism (no internal stress or backstress),<sup>[15]</sup> with dislocations easily reversing their motion across cells. Sleeswyk *et al.* suggested that gliding dislocations, during work hardening, encounter increasingly effective obstacles, and the stress necessary to activate further dislocation motion or plasticity continually increases. On reversal of the direction of straining, however, the dislocations, initially, will need to only move past those obstacles they have already surmounted. Thus, the flow stress is initially relatively low. High-temperature work by Hasegawa *et al.*<sup>[16]</sup> suggested that dissolution of the cell/subgrains occurred with a reversal of the strain, indicating an “unraveling” of the substructure in Cu-16 at pct Al, perhaps consistent with the ideas of Sleeswyk and co-workers.

There are two broad theories for the basis of backstresses or internal stresses that can also rationalize the Bauschinger effect. In a fairly influential development, Mughrabi<sup>[17,18]</sup> advanced the concept of relatively high internal stresses in subgrain walls and cell structures. He advocated the simple case where “hard” (high-dislocation-density walls or cells) and soft (low-dislocation-density cell or subgrain interior) elastic–perfectly plastic regions are compatibly sheared in parallel. Each component yields at different stresses and, hence, the composite is under a heterogeneous stress state, with the cell walls (subgrains at high temperatures) having the higher stress. This leads to an interpretation involving an inhomogeneous stress state and backstresses. This composite may also rationalize the Bauschinger effect. As the hard and soft regions are unloaded in parallel, the hard region eventually (while the stress in the hard region is still positive) places the soft region in compression, leading to a backstress. The “total” or “average” stress may be zero, while the stress in the hard region can be positive and negative in the soft region. Thus, a Bauschinger effect can be observed, where plasticity occurs on reversal at a lower average magnitude of stress than that on initial unloading. This “composite” model appears to have been embraced by Derby and Ashby,<sup>[19]</sup> Blum and co-workers,<sup>[13,20]</sup> Nix and co-workers,<sup>[1,21]</sup> as well as many others (*e.g.*, References 22 through 25) for creep. This model is illustrated in Figure 2.

*In-situ* deformation experiments by Lepinoux and Kubin<sup>[26]</sup> and the well-known neutron irradiation experiments by Mughrabi<sup>[17]</sup> measured dislocation-loop radii near dipole bundles (heterogeneities). These suggested internal stresses that are, roughly, a factor of 3 higher than the applied stress during cyclic deformation of Cu at ambient temperature. More recent experiments measuring the heights of dislocation dipoles by Kassner *et al.*<sup>[27]</sup> on cyclically deformed Al and Cu allowed an estimate of the stress at different locations in the substructure during deformation. It was concluded that the stress state appeared nearly uniform across the dislocation substructure and was also about *equal* to the applied stress. Morris and Martin<sup>[22,23]</sup> concluded that dislocations are ejected from sources at the subgrain boundary by high local stresses. High local stresses, perhaps a factor of 20 higher than the applied stress, were concluded by observing the radius of curvature of “ejecting dislocations” “frozen in place” (amazingly) by a precipitation reaction in Al-5 at. pct Zn on cooling from the creep temperature. Stress-dip tests have often been interpreted to suggest internal stresses.<sup>[24,28,29]</sup>

Another concept of backstress is related to dislocation configurations. This was proposed by Argon and Takeuchi,<sup>[25]</sup> Gibeling and Nix,<sup>[21]</sup> and Nix and Ileschner.<sup>[1]</sup> With this model, the subgrain boundaries that form from a dislocation reaction bow under action of the shear stress, and this creates relatively high “long-range” internal stresses. The high stresses in the vicinity of the boundary are suggested to be roughly a factor of 3 larger than the applied stress. On unloading, a negative stress in the subgrain interior causes reverse plasticity (or anelasticity). There is a modest anelastic backstrain that is associated with this backstress.

One of the more recent investigations in this area of internal stresses was performed by Straub *et al.*<sup>[13]</sup> and Borbély *et al.*<sup>[30,31]</sup> This work consisted of X-ray diffraction (XRD)

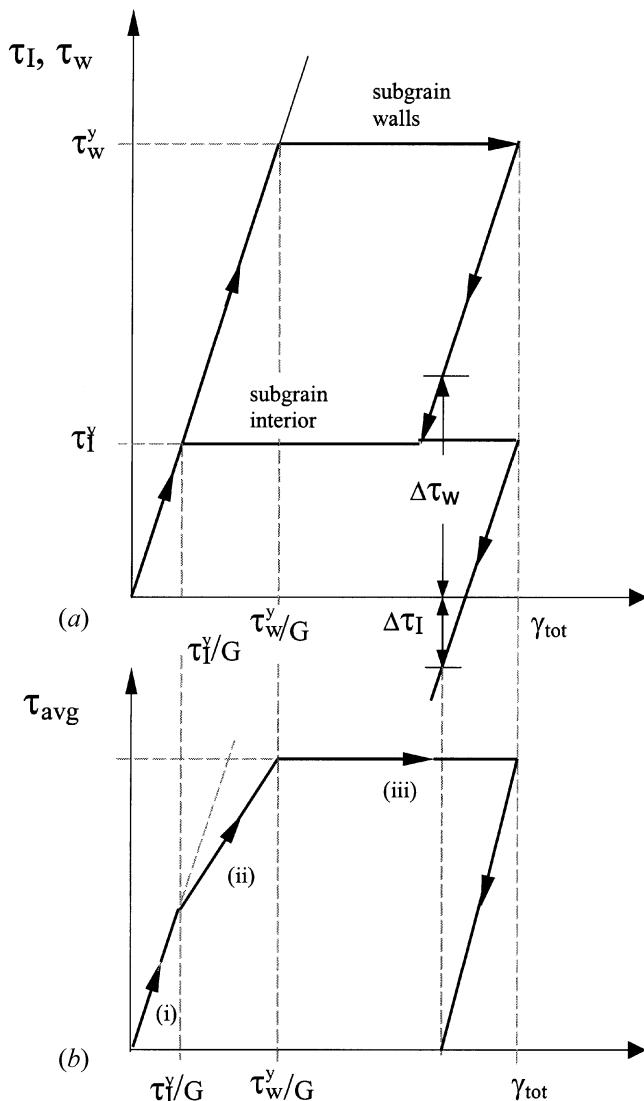


Fig. 2—The composite model illustrating backstresses. (a) The different stress vs strain behaviors of the (hard) subgrain walls and (soft) subgrain interiors and (b) the stress vs strain behavior of the composite. When the composite is completely unloaded, the subgrain interior is under compressive stress. This leads to yielding of the softer component in compression at a macroscopic stress lower than  $\tau_i^y$  under initial loading. Hence, a Bauschinger effect due to inhomogeneous (or internal) stress is observed.

and convergent-beam electron diffraction (CBED) of specimens creep tested to steady state. Some X-ray test experiments were performed *in situ*, or while the creep specimen was under stress. Basically, X-ray peaks broaden with plastic deformation. A “deconvolution” is performed, which results in two nearly symmetric peaks. One peak is suggested to represent the small amount of metal in the vicinity of subgrains, where high local stresses are presumed to increase the lattice parameter. This physical interpretation of the diffraction results has been questioned by others.<sup>[32]</sup> A CBED on thin foils can probe smaller areas (beam size less than 100 nm) rather than the entire sample, as with X-rays, and is potentially reasonably accurate in assessing local internal stresses. The results by Borbély *et al.*, which suggest high local stresses in the vicinity of subgrain boundaries in copper, based on CBED, however, may be speculative, as the results in Figure 3 of Reference 30 are ambiguous. Basically, both

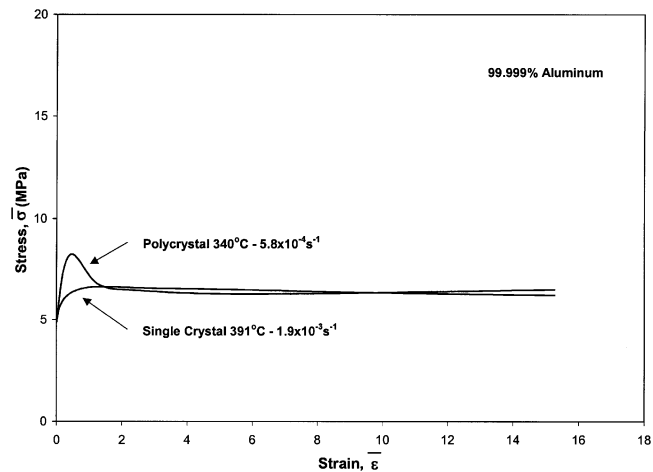


Fig. 3—The equivalent uniaxial stress of Al single crystal ( $\langle 111 \rangle$  parallel to torsion axis) vs strain. A polycrystalline specimen is also illustrated.<sup>[33]</sup>

sets of experiments (XRD and CBED) are, nonetheless, interpreted by the investigators to suggest that the lattice parameters within the specimens are larger near subgrain (and cell) walls than in the subgrain interior. These are important experiments.

In the present work, CBED was performed on aluminum single crystals and, especially, on copper polycrystals that were creep tested within the five-power-law creep regime. The objective was to probe the subgrains to determine whether any changes in the lattice parameter are observed near walls, which would indicate the presence of an internal stress. A subgrain boundary is relatively thin (*e.g.*, 3b) with a relatively high misorientation ( $>1$  deg), while cellular structures are thicker, with lower misorientations ( $<1$  deg). Thus, examining each of these types of boundaries or walls for high local stresses was considered desirable.

## II. EXPERIMENTAL PROCEDURE

Copper polycrystals of 99.9985 pct purity, provided by The Metron Group, were first annealed in vacuum at  $8 \times 10^{-4}$  Torr and 1000 °C for 10 hours at the Albany Research Center (Albany, OR). The resulting grain size was about 0.42 mm. Testing was performed on a Satec creep testing machine at Oregon State University with high-purity argon atmosphere. Tests were performed at two constant stresses, and the loads were altered to account for changes in cross-sectional area. Cu specimens were quenched within 5 seconds after creep testing. The mechanical procedures for Al were reported earlier by the authors in References 33 and 37.

The Al single crystals were deformed in torsion to an equivalent uniaxial strain of about 3.6 at 391 °C at an equivalent uniaxial strain rate of  $1.9 \times 10^{-3} \text{ s}^{-1}$ , using the Stanford torsion machine. Specimens were quenched immediately upon termination of the test. The stress vs strain behavior is shown in Figure 3 along with the polycrystalline behavior.<sup>[33]</sup> The crystals were provided by The Metron Group, and the  $[111]$  direction was parallel to the torsion axis. The average subgrain size was measured to be 15.3  $\mu\text{m}$  in a similar specimen deformed to a strain of 16.3.<sup>[33]</sup> The typical misorientation of subgrain boundaries measured by selected-area electron diffraction was 1 to 2 deg. About 10 pct of subgrain

boundaries were high-angle ones ( $8 \text{ deg} < \theta < 62 \text{ deg}$ ), with a typical value of about  $20 \text{ deg}$ . These were concluded to have been formed from a dislocation reaction, possibly as geometric necessary boundaries,<sup>[34]</sup> rather than by discontinuous DRX.

Copper and aluminum foils were electropolished in a Fischione twin jet; for the Cu disks, 10 pct nitric acid and 90 pct methanol at  $-25 \text{ }^{\circ}\text{C}$  were used, and for the Al disks, 5 pct perchloric acid, 20 pct butoxyethanol, and 75 pct methanol at  $-25 \text{ }^{\circ}\text{C}$  were used. The Cu and Al foils were examined under bright-field conditions using a PHILIPS\*

\*PHILIPS is a trademark of Philips Electronic Instruments Corp., Mahwah, NJ.

EM 400 transmission electron microscope (TEM) at 120 kV, located at the University of California at San Diego.

The microstructure characterization included the average subgrain-boundary misorientation ( $\theta$ ), average density of dislocations not associated with subgrain boundaries ( $\rho$ ), and average subgrain intercept ( $\lambda$ ). The misorientation of a subgrain boundary is defined as the minimum angle of rotation that is necessary to bring the two crystals separated by the boundary into coincidence. This was determined using Kikuchi line shifts across a boundary using a single orientation to the foil that accurately estimates the amount of tilt of a boundary (the low-rotation component of the misorientation of low-angle ( $<1 \text{ deg}$ ) boundaries is nearly indiscernible by this procedure). The average subgrain-boundary misorientations were calculated from ten different measurements for Cu (and from about 65 for Al). The density of dislocations not associated with boundaries was determined using the surface intersection technique,<sup>[35]</sup> using, typically, 20 micrographs. The  $\langle 220 \rangle$  two-beam conditions were used to image dislocations in Cu. The region of the foils from which  $\rho$  was determined in Cu was  $0.2 \text{ }\mu\text{m}$  in thickness. The subgrain sizes in Cu were measured as an average intercept based on several montages of, typically, 10 micrographs each at about 13,000 times magnification, based on several foils.

The CBED was performed using a  $\langle 411 \rangle$  zone axis. Second-order HOLZ lines were used. For aluminum, the accuracy of the lattice-parameter measurements was about  $\pm 0.00005 \text{ nm}$ , or about  $\pm 0.01 \text{ pct}$ . The accuracy of lattice-parameter measurements for Cu was about  $\pm 0.0001 \text{ nm}$ , or  $\pm 0.03 \text{ pct}$ . The error associated with lattice-parameter measurements is based on the quality of the CBED pattern. The CBED examination was performed at  $-175 \text{ }^{\circ}\text{C}$ . The CBED beam diameter was estimated to be  $80 \text{ nm}$ . A large C2 aperture,  $250 \text{ }\mu\text{m}$  in diameter, was utilized, which allowed a large angular view of the diffraction spots. The CBED patterns were simulated using the software DF Tools 5.1.<sup>[36]</sup>

### III. RESULTS

The Al single crystals were deformed in torsion to an equivalent uniaxial strain of about 3.6 at  $391 \text{ }^{\circ}\text{C}$  at an equivalent uniaxial strain rate of  $1.9 \times 10^{-3} \text{ s}^{-1}$ . The stress vs strain behavior is shown in Figure 3, along with the polycrystalline behavior. The single crystal was deformed to steady state at a temperature and strain rate corresponding to well within the five-power-law regime.<sup>[9]</sup> Six subgrain boundaries in two TEM foils were traversed using CBED. Figure 4 is a TEM micrograph that shows the locations of some of the measurements. Figure 5 shows the lattice-parameter measurements

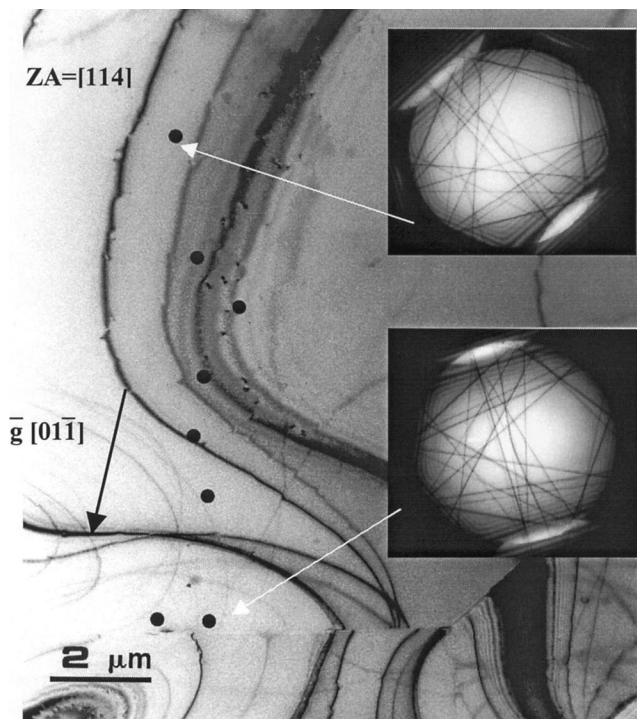


Fig. 4—A TEM micrograph depicting the locations of CBED determinations within an aluminum single-crystal subgrain. The CBED patterns refer to two locations, one near a boundary and one well within the interior.  $\langle 411 \rangle$  zone axis.

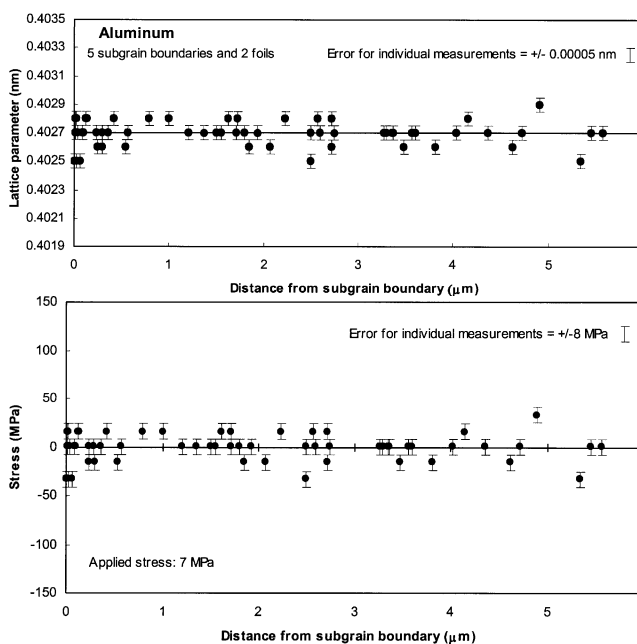


Fig. 5—The lattice parameter and corresponding stress determinations based on the CBED in a single crystal of Al deformed to steady state within the five-power-law creep regime. The error bracket refers to the error associated with uncertainties of a lattice parameter measurement. Some scatter of the data possibly due to the presence of bend contours is also evident.

and residual-stress calculations. It was determined that the lattice parameter was unchanged within the interior of the subgrain and along the boundaries, within a one-beam diameter (or  $80 \text{ nm}$ ) of the subgrain boundary. The measurements

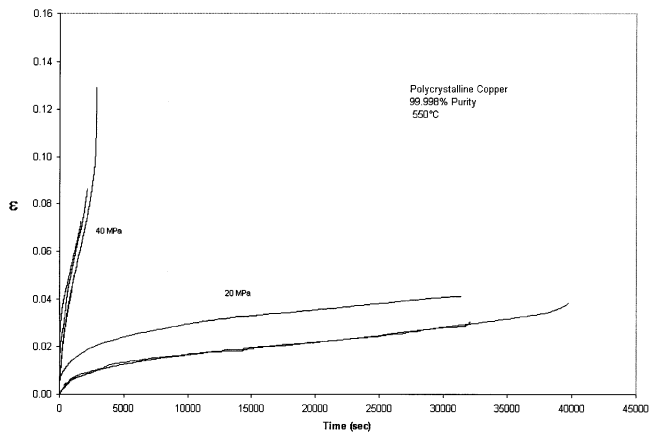


Fig. 6—The strain (plastic) vs time for copper deformed at 550 °C at 20 and 40 MPa.

were also identical to those of the annealed, stress-free Al polycrystals. Thus, the deformed substructure is stress free within the accuracy of the lattice-parameter measurements of CBED. The (residual) stress-measurement error is approximately  $\pm 8$  MPa, or a value nearly equal to the applied stress. There appears to be scatter in the Al experiments, aside from the error associated with lattice-parameter measurements in the CBED patterns (about  $\pm 0.00005$  nm, or  $\pm 0.01$  pct). These are possibly due to bend contours that are visible in the micrograph. These Al results are also being reported in a proceedings.<sup>[33]</sup>

Six (of ten) of the copper polycrystalline specimen creep tests are illustrated in Figure 6. Tests were performed at 550 °C at a 20 and 40 MPa constant true stress. The work by Barrett *et al.*<sup>[2]</sup> suggests that the low-stress tests are well below the regime for DRX, while the high-stress tests are only slightly below the regime. Pahutova *et al.*<sup>[5]</sup> suggest that DRX does not occur below about 750 °C. The tests in Figure 6 appear to show the typical three stages of creep for pure metals. None of the tests indicated evidence of “undulations” which may signify DRX. A steady state was achieved within a few percentages of strain. These data are summarized in Figure 1 and are consistent with earlier works in terms of the power-law stress exponent. The somewhat lower values of strain rate, compared to other studies, are not understood, although particular care was exercised in the present study to maintain constant stress. (The two points on Figure 1 for this study represent the average steady-state values of ten tests.)

The gage and grip sections were examined by optical metallography, and the grains appeared of identical size in both regions for both the high- and low-stress specimens. Closer inspection of the higher-stress specimens revealed occasional small (*e.g.*, 10  $\mu\text{m}$ ) grains on boundaries of grains typically 1000  $\mu\text{m}$  in diameter. These features did not appear in the grip section. Thus, some DRX appears to have occurred in the vicinity of some high-angle boundaries of the high-stress specimen, although these did not affect the measured dislocation microstructure (statistically, at the interior of grains) or mechanical characterization. The behavior appears to be dominated by dynamic recovery. One additional possibility is oxidation within the grains (although not observed by others<sup>[10]</sup>), as evidenced by optical metallography.

The steady-state dislocation substructure is summarized in Table I. The data were taken from specimens tested to steady state and quenched. First, subgrains are formed, as evidenced by a misorientation usually not evident in a cellular substructure. An example of this substructure is illustrated in Figure 7. The boundaries, however, do not appear to be of as high a misorientation as, nor as well defined as, subgrains in both high- and low-stacking-fault-energy metals and alloys<sup>[9]</sup> at steady state. Hence, these boundaries in Cu are referred to as “less-well-defined subgrain boundaries.” Whether impurities, such as absorbed oxygen, introduced during these tests lead to this decrease in definition is unknown.

Five subgrain boundaries in three Cu TEM foils were traversed using CBED. The foils were extracted from specimens deformed at each of the two stresses to steady state. Figure 7 is a TEM micrograph that shows the typical microstructure from which measurements were extracted. Figures 8(a) and (b) show the lattice-parameter and residual-stress calculations. It was determined that the lattice parameter was unchanged within the interior of the subgrain and along the boundaries, within a one-beam diameter (or 80 nm) of the subgrain boundary. The measurements were also identical to those of the annealed, stress-free Cu polycrystals. Thus, within the accuracy of the lattice-parameter measurements of CBED, the creep-deformed Cu substructure is stress free. The (residual) stress error associated with the strain measurements is approximately  $\pm 30$  MPa, again, about equal to the applied stress.

Of course, it must be considered possible that some, relatively small, residual stresses are present, but too small to be detected by CBED, or that residual stresses were once present but relaxed to an undetectable level in both Al and Cu. Several earlier investigations referenced, as mentioned previously, suggest that stresses may be high in the vicinity of the so-called hard subgrain boundaries. The (presumed) internal stresses based on asymmetric X-ray peaks were found to only partially relax on unloading and were detectable in (bulk) specimens in the unloaded condition.<sup>[31]</sup> Hence, if internal stresses are actually being measured by X-rays, such as with the referenced investigations, they could be detected in unloaded TEM thin foils using CBED, but they are not. In Al, for instance, the dislocation substructure does not appear to recover in foils thinned to about 1  $\mu\text{m}$ .<sup>[37]</sup> The dislocation substructure appears identical to those where the structure is “pinned” by precipitation (*e.g.*, Al 5 at. pct Zn). Thus, it appears that any recovery of the internal stress in the thinning process only can occur at thicknesses less than 1  $\mu\text{m}$ . The maximum amount of recovered elastic stress from the network (interior to the subgrain) by dislocation ejection from the foil can be estimated to be less than the applied stress. It is unknown to what degree dislocations are ejected from the subgrain boundary, although there is no direct evidence of such dislocation ejection. The dislocation density, in the region where the CBED measurements in the high-stress Cu specimen were performed, was  $2.0 \times 10^9 \text{ cm}^{-2}$ . The dislocation density was  $0.8 \times 10^9 \text{ cm}^{-2}$  where CBED was performed in the low-stress specimen foils. These are quite similar to the values in the thickest regions, listed in Table I. Thus, it appears, within the error of the measurements, that recovery of the dislocation substructure does not occur in those regions where CBED is performed, as

**Table I. The Steady-State Dislocation Substructure of Creep-Deformed Copper at 550 °C**

Steady-State Stress (MPa)	Strain	Average Misorientation (Deg)	Average Dislocation Density (Not Associated with Boundaries) ( $\text{cm}^{-2}$ )	Average Subgrain Intercept ( $\mu\text{m}$ )	Steady-State Strain Rate ( $\dot{\epsilon}_{ss}, \text{s}^{-1}$ )
40	0.05	0.23	$1.65 \times 10^9$	1.5	$2.5 \times 10^{-5}$
20	0.04	0.09	$1.2 \times 10^9$	3.1	$5.6 \times 10^{-7}$

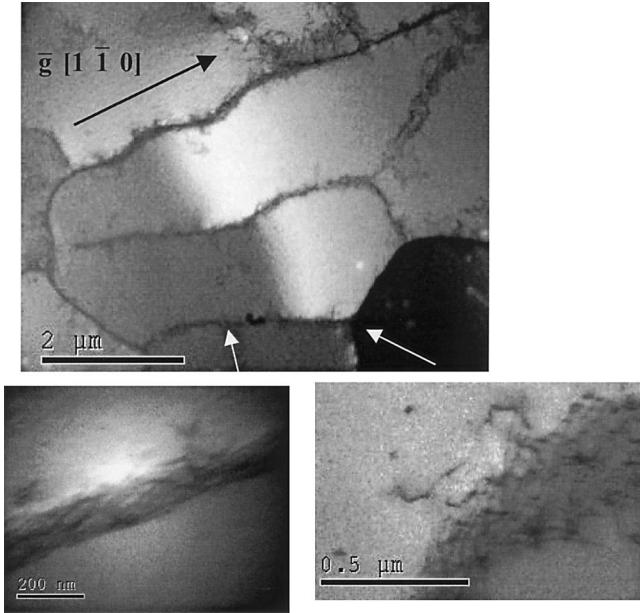


Fig. 7—TEM micrograph illustrating the typical subgrain microstructure of polycrystalline Cu deformed at 20 MPa and 550 °C to a strain of approximately 0.04.

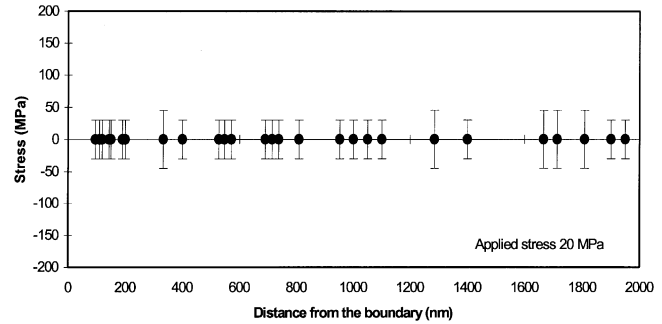
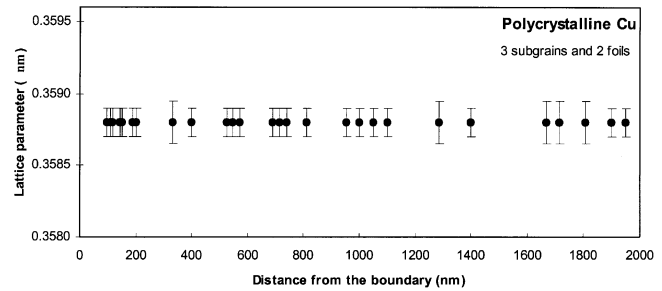
compared to those relatively thick regions where the dislocation density measurements are performed ( $0.2 \mu\text{m}$ ) in Cu. Thus, if high internal stresses are present in creep-deformed specimens and are not substantially recovered on unloading, as suggested by internal-stress proponents, then thin-foil CBED examination should allow detection of these stresses. None are observed by CBED.

Figures 8 and 9 plot the subgrain size and dislocation-density data of Table I and are reasonably consistent with the expected trends for the network dislocation density vs the modulus-compensated steady-state stress and the average subgrain intercept vs modulus-compensated steady-state stress, in view of the limited data. Compilation of large quantities of data for other metals<sup>[9]</sup> suggests that

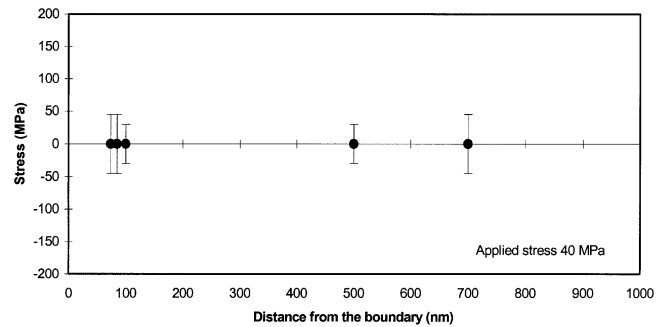
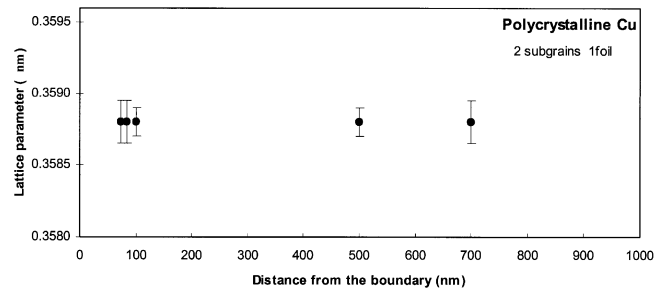
$$\left(\frac{\sigma_{ss}}{G}\right) = C_1 \left(\frac{1}{\lambda}\right)^{-1} \quad [1]$$

$$\left(\frac{\sigma_{ss}}{G}\right) = C_2 \rho^p \quad [2]$$

where  $C_1$  and  $C_2$  are constants. These values are indicated in the figures. The subgrain exponent of the figure is consistent with Eq. [1], but the value of  $p$  for Eq. [2] is consistent with the range of exponents observed in different metals, considering the scatter of values in the literature and the limited data of the present study. The value, here, of  $p$  is somewhat higher than the typical value of 0.5.



(a)



(b)

Fig. 8—The lattice parameter and corresponding stress based on the CBED performed at locations very near subgrain walls and interior to the subgrains in polycrystalline Cu deformed to steady state within the five-power-law creep regime at (a) 20 and (b) 40 MPa to strains of 0.04 and 0.05, respectively.

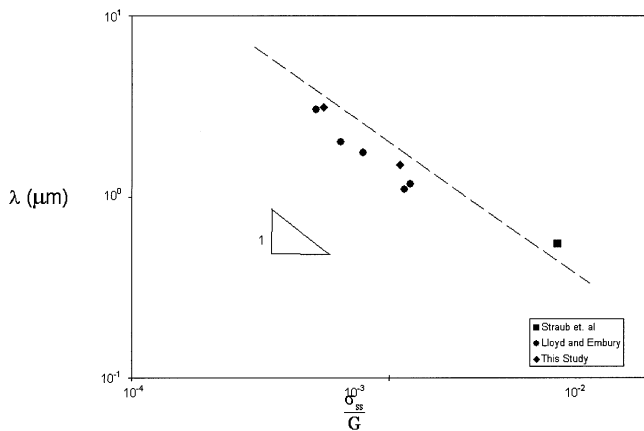


Fig. 9—The steady-state modulus-compensated stress vs the steady-state subgrain size in Cu. A line of slope one is indicated, which is the expected behavior based on other materials. The strains are 0.04 and 0.05 for the low and high stresses, respectively.

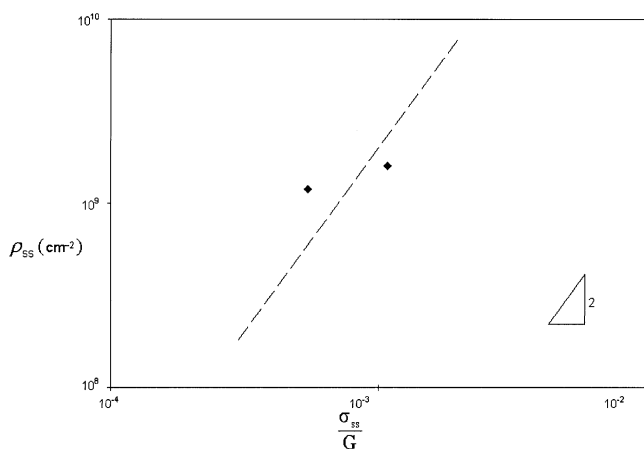


Fig. 10—The steady-state modulus-compensated stress vs the steady-state density of dislocations (not associated with subgrain boundaries) for Cu. The strains are 0.04 and 0.05, respectively.

#### IV. CONCLUSIONS

Al single crystals and Cu polycrystals were deformed to steady state within the five-power-law regime. It was found that the microstructure of Cu consists of less-well-defined subgrain boundaries than Al and other metals within the five-power-law regime, consistent with many earlier investigations. The CBED measurements were performed in Al single crystals and Cu polycrystals to measure internal stresses. Several subgrains were transversed from one subgrain boundary to the opposite side in multiple TEM foils. It was determined that there were no detectable internal stresses either near the well-defined Al and less-well-defined Cu subgrain walls or within the subgrain interiors.

#### ACKNOWLEDGMENTS

The authors acknowledge support from the Northwest Aluminum Professorship and the United States Department

of Energy Basic Energy Sciences under Contract No. DE-FG03-99ER45768. The authors are grateful for the help by Mark Wall, ML Tech. The authors are also grateful to the Albany Research Center for assistance with annealing. The assistance of Professor B. Wilshire is greatly appreciated.

#### REFERENCES

1. W.D. Nix and B. Ilshner: *Strength of Metals and Alloys*, P. Haasen, V. Gerold, and G. Kostorz, Pergamon, Oxford, United Kingdom, 1980, pp. 1503-30.
2. C.R. Barrett and O.D. Sherby: *Trans. AIME*, 1964, vol. 230, pp. 1322-27.
3. C.R. Barrett, Lytton, and O.D. Sherby: *Trans. AIME*, 1967, vol. 239, pp. 170-84.
4. D.J. Lloyd and J.D. Embury: *Met. Sci.*, 1970, vol. 4, pp. 6-8.
5. Pahutova, J. Cadek, and P. Rys: *Phil. Mag.*, 1971, vol. 23, pp. 509-17.
6. S.V. Raj and T.G. Langdon: *Acta Metall.*, 1989, vol. 37, pp. 843-52.
7. J.D. Parker and B. Wilshire: *Mater. Sci. Eng.*, 1980, vol. 43, pp. 271-80.
8. J.D. Parker and B. Wilshire: *Met. Sci.*, 1978, vol. 12, pp. 453-58.
9. M.E. Kassner and M.T. Perez-Prado: *Progr. Mater. Sci.*, 2000, vol. 45, pp. 1-102.
10. B. Wilshire: Nashville, TN, private communication, 2000.
11. M.R. Staker and D.L. Holt: *Acta Metall.*, 1972, vol. 20, pp. 509-89.
12. S.V. Raj and R.G. Langdon: *Acta Metall.*, 1991, vol. 39, pp. 1823-32.
13. S. Straub, W. Blum, H.J. Maier, T. Ungar, A. Borberly, and H. Renner: *Acta Mater.*, 1996, vol. 44, pp. 4337-50.
14. A.W. Sleeswyk, M.R. James, D.H. Plantinga, and W.S.T. Maathuis: *Acta Metall.*, 1978, vol. 126, pp. 1265-71.
15. E. Orowan: *Internal Stress and Fatigue in Metals*, General Motors Symp., Elsevier, Amsterdam, 1959, p. 59.
16. T. Hasegawa, Y. Ikeuchi, and S. Karashima: *Met. Sci.*, 1972, vol. 6, pp. 78-82.
17. H. Mughrabi: *Acta Metall.*, 1983, vol. 31, pp. 1367-79.
18. H. Mughrabi: *Mater. Sci. Eng. A*, 1987, vol. 85, pp. 15-31.
19. B. Derby and M.F. Ashby: *Acta Metall.*, 1978, vol. 35, pp. 1349-53.
20. W. Blum, A. Cegielska, A. Rosen, and J.L. Martin: *Acta Metall.*, 1989, vol. 37, pp. 2439-53.
21. J.C. Gibeling and W.D. Nix: *Acta Metall.*, 1980, vol. 29, pp. 1769-84.
22. M.A. Morris and J.L. Martin: *Acta Metall.*, 1984, vol. 32, pp. 1609-23.
23. M.A. Morris and J.L. Martin: *Acta Metall.*, 1984, vol. 32, pp. 549-61.
24. S. Karashima, T. Iikubo, T. Watanabe, and H. Oikawa: *Trans. Jpn. Inst. Met.*, 1971, vol. 12, pp. 369-74.
25. A.S. Argon and S. Takeuchi: *Acta Metall.*, 1981, vol. 29, pp. 1877-84.
26. Lepinoux and L.P. Kubin: *Phil. Mag. A*, 1985, vol. 57, pp. 675-96.
27. M.E. Kassner, M.-T. Pérez-Prado, K.S. Vecchio, and M.A. Wall: *Acta Mater.*, 2000, vol. 48, pp. 4247-54.
28. C.N. Ahlquist and W.D. Nix: *Acta Metall.*, 1971, vol. 19, pp. 373-85.
29. W. Blum, J. Hausselt, and G. König: *Acta Metall.*, 1976, vol. 24, pp. 293-97.
30. Borbély, G. Hoffmann, E. Aernoudt, and T. Ungar: *Acta Mater.*, 1997, vol. 45, pp. 89-98.
31. Borbély, W. Blum, and T. Ungar: *Mater. Sci. Eng.*, 2000, vol. 276, pp. 186-94.
32. I. Gaal: *Proc. 5th Int. Riso Symp.*, N. Hessel Andersen, M. Eldrup, N. Hansen, D. Juul Jensen, T. Leffers, H. Lilholt, O.B. Pedersen, and B.N. Singh, eds., Riso National Lab., Roskilde, Denmark, 1984, pp. 249-54.
33. M.E. Kassner, M.T. Pérez-Prado, and K.S. Vecchio: *Mater. Sci. Eng.*, in press.
34. R.D. Doherty, D.A. Hughes, F.J. Humphreys, J.J. Jonas, D. Juul Jensen, M.E. Kassner, W.E. King, T.R. McNelley, H.J. McQueen, and A.D. Rollett: *Mater. Sci. Eng.*, 1997, vol. A238, pp. 219-74.
35. P.B. Hirsch, A. Howie, R.B. Nicholson, and D.W. Pashley: *Electron Microscopy of Thin Crystals*, Butterworth and Co., London, 1965, p. 422.
36. J. Sutliff: Lehigh University, Bethlehem, PA, 1985.
37. M.E. Kassner and M.E. McMahon: *Metall. Trans. A*, 1987, vol. 18A, pp. 835-46.
38. O.D. Sherby and P.M. Burke: *Progr. Mater. Sci.*, 1967, vol. 13, pp. 325-90.